Available online at www.sciencedirect.com
ScienceDirect
Chemical Physics Letters 448 (2007) 41–45
CHEMICAL PHYSICS LETTERS
www.elsevier.com/locate/cplett

Temperature dependence of hydrated La^{3+} properties in liquid water, a molecular dynamics simulations study

Magali Duvail [a,*], Riccardo Spezia [a], Thierry Cartailler [a], Pierre Vitorge [a,b]

[a] *Laboratoire Analyse et Modélisation pour la Biologie et l'Environnement, CNRS UMR 8587, Université d'Evry Val d'Essonne, Boulevard F. Mitterrand, 91025 Evry Cedex, France*
[b] *CEA Saclay, DEN/DPC/SECR/LSRM, 91991 Gif Sur Yvette, France*

Received 15 June 2007; in final form 19 September 2007
Available online 25 September 2007

Abstract

La^{3+} hydration was studied in the 277–623 K temperature range by molecular dynamics simulations using explicit polarization. Although temperature has virtually no effect on the first hydration shell structural properties, dynamical properties are temperature dependent. Equilibrium constants are deduced from the $La(H_2O)^{3+}_{(i-1)}/La(H_2O)^{3+}_{i}$ population ratios. The reactions are enthalpy driven, and $\Delta_r H^0_{i,298}$ decreases with i. All these results are consistent with a quite rigid first hydration shell.

1. Introduction

Lanthanide trications (Ln^{3+}) hydrations have been extensively studied by means of classical molecular dynamics (CLMD) at room temperature [1–10]. CLMD simulations can give realistic pictures of hydrated ion structures and dynamics with a relatively low computational cost for simulations of up to nanoseconds, a time scale enough to study exchanges of water molecules in the Ln^{3+} hydration shells.

Some experimental studies recently appeared on the influence of temperature on the stabilities of aqueous hydroxides and complexes of f-block elements [11–14]. In particular, Lindqvist et al. have studied temperature dependency of Cm^{3+} hydration by time-resolved laser fluorescence spectroscopy (TRLFS) [11]. They concluded that the $Cm(H_2O)^{3+}_8/Cm(H_2O)^{3+}_9$ equilibrium is entropy driven ($-298\ \Delta_r S^0_{i,298} = 7.6 \pm 0.4\ \text{kJ mol}^{-1}$), although their enthalpic contribution value ($-13 \pm 0.4\ \text{kJ mol}^{-1}$) is actually more important at room temperature. In the late 80s Miyakawa et al. [15] have calculated virtually the same entropic contribution for the whole Ln series: $-298\ \Delta_r S^0_{9,298} = 10\ \text{kJ mol}^{-1}$, while the enthalpy changes vary along the Ln series, which is consistently attributed to the Ln contraction. Note that they report the same value of $\Delta_r G^0_{9,298}$ ($5\ \text{kJ mol}^{-1}$) for La^{3+} and Ce^{3+}.

In the present work we report for the first time a systematic molecular dynamics study of the temperature influence on La^{3+} hydration using our recently developed La^{3+}–water pair interaction potential including explicit polarization [10,16]. The La^{3+} ion – first element in the lanthanide series – was chosen to simplify the quantum chemistry calculations used to parametrize the pair interaction potential, since La^{3+} has the simplest electronic configuration in the lanthanide series, *i.e.* closed-shell with no f-electron.

2. Computational details

The total energy of our system is modelled as a sum of potential terms:

$$V_{\text{tot}} = V_{\text{elec}} + V^{\text{LJ}}_{\text{O–O}} + V_{\text{La–O}}, \tag{1}$$

where V_{elec} is the electrostatic energy term composed of a Coulomb and a polarization terms following the Thole's induced dipole model [17]. $V^{\text{LJ}}_{\text{O–O}}$ is a 12-6 Lennard-Jones

* Corresponding author. Fax: +33 (0)1 69 47 76 55.
E-mail address: magali.duvail@gmail.com (M. Duvail).

0009-2614/$ - see front matter © 2007 Elsevier B.V. All rights reserved.
doi:10.1016/j.cplett.2007.09.059

potential describing the O–O interaction for which we used a modified TIP3P/P model [10,18], where the charges on O and H were rescaled. $V_{\mathrm{La-O}}$ account for the *non-electrostatic* La–O interactions, modelled with an exponential-6 Buckingham potential [19]. The Buck-6 parameters were based on *ab initio* calculations at the MP2 level of theory using the LanL2MB basis set for La [20–22] and 6-31G* [23] for H and O.

MD simulations have been carried out in the microcanonical ensemble with our own developed CLMD code [16] for one La^{3+} and 216 rigid water molecules in a cubic box. The size of the cubic box was adjusted to reproduce the density of pure liquid water at different temperatures (in the 277–623 K range) [24]. The volume change due to La^{3+} was neglected, since some simulations were performed taking into account the La^{3+} volume and the same results were obtained. The La^{3+} volume, estimated from the ionic radius [25], is indeed 7.53 $Å^3$, corresponding to 0.1% of the smallest box volume (6460.73 $Å^3$ at 274 K). Periodic boundary conditions were applied to the simulation boxes. Long-range interactions have been calculated by using the smooth particle mesh Ewald (SPME) method [26]. Simulations were performed using a velocity-verlet-based multiple time scale (MTS) using a 1 fs time step for positions and velocities and 5 fs for dipole dynamics. The system was first equilibrated at the target temperature for 2 ps, and then production runs were collected for 3 ns. The average temperature range were 274–624 K with a standard deviation of 9–17 K, respectively.

3. Thermodynamics analysis

The Gibbs energies changes of the

$$\mathrm{La(H_2O)}_{i-1}^{3+} + \mathrm{H_2O} \rightleftharpoons \mathrm{La(H_2O)}_{i}^{3+} \tag{2}$$

water exchange reactions were calculated from

$$K_{i,T}^{0} = \frac{a_i}{a_{i-1} \cdot a(\mathrm{H_2O})} \tag{3}$$

where $a(\mathrm{H_2O}) = 1$ at any temperature, the usual definition for the activity of water, and a_i is the activity of $\mathrm{La(H_2O)}_{i}^{3+}$. We used the $a_i/a_{i-1} = C_i/C_{i-1}$ approximation, where C_i is the $\mathrm{La(H_2O)}_{i}^{3+}$ concentration, and $C_i/C_{i-1} = n_i/n_{i-1}$, where n_i is the number of $\mathrm{La(H_2O)}_{i}^{3+}$ configurations. This type of ratio is indeed currently interpreted in term of equilibrium constant [11]. However this is based on several assumptions: (i) $C_i/C_{i-1} = a_i/a_{i-1}$; this is valid for infinite dilution, namely no La^{3+}–La^{3+} interactions, (ii) the $K_{i,T} = C_i/C_{i-1}$ ratio is interpreted as the equilibrium constant of Reaction (2), and (iii) the effects of the T and P variations are neglected during each simulation. The classical thermodynamic equation

$$\mathrm{R}\ln(K_{i,T}^{0}) = \mathrm{R}\ln(K_{i,T^0}^{0}) - \Delta_r H_{i,T^0}^{0}\left(\frac{1}{T} - \frac{1}{T^0}\right) - \frac{1}{T}\int_{T^0}^{T} \Delta_r C_{p,i}\,\mathrm{d}T + \int_{T^0}^{T} \frac{\Delta_r C_{p,i}}{T}\,\mathrm{d}T - \frac{1}{T}\int_{P^0}^{P} \Delta_r V_{\mathrm{m},i}\,\mathrm{d}P \tag{4}$$

was used to estimate the systematic error originated in these approximations, where $\Delta_r C_{p,i}$ is the heat capacity change, and $\Delta_r V_{\mathrm{m},i}$ the molar volume change for the same reaction. To check that pressure variations could be neglected, we performed a simulation at 624 K with a density of 0.997 instead of 0.589, *i.e.* the density of the liquid/gas curve. 0.997 is the density at 298 K. At 624 K we obtained $\log(K_9) = 1.68 \pm 0.19$ and 1.41 ± 0.46, for $d = 0.997$ and 0.589, respectively. Note that with this relatively large uncertainties the two equilibrium constants are not clearly separated, such that, in the range we have investigated, pressure effects are well inside the available uncertainties. $\Delta_r H_{i,T}^{0}$, $\Delta_r S_{i,T}^{0}$ and $\Delta_r G_{i,T}^{0}$, the thermodynamic parameters for Reaction (2) were obtained from the van't Hoff approximation.

The chemical potential of water, $\mu_{\mathrm{H_2O}}^{0}$, has a contribution to

$$\Delta_r G_{i,T}^{0} = \mu_i^0(T) - \mu_{i-1}^0(T) - \mu_{\mathrm{H_2O}}^0(T) \tag{5}$$

where $\mu_i^0(T)$ is the standard chemical potential of species $\mathrm{La(H_2O)}_{i}^{3+}$ at temperature T [24]. To plot this contribution, we define $\Delta_T\mu = \mu_i^0(T) - \mu_i^0(298)$.

4. Results and discussion

4.1. Structural and dynamical properties

Increasing the temperature has very small effect on the position of the first hydration shell, whereas a slight shift in the position of the second hydration shell is observed (Table 1). The peak widths increase with temperature for the first and the second hydration shells (see Fig. 1). A slight increase of the CN is observed: for instance at 274 K, our first shell value of 9.00 is an average of different distributions of complexes with CN = 9 (99.6%) and 10 (0.4%), and at 624 K, the most frequent coordination number is still 9 but with other distributions, namely 3.2% for CN = 8, 84.3% for CN = 9 and 12.5% for CN = 10 (Table 2). Note that for each temperature, the CN is an average of different distributions of complexes $\mathrm{La(H_2O)}_{i}^{3+}$ ($i = 8$–11) (Fig. 2). For the main stoichiometry $\mathrm{La(H_2O)}_{9}^{3+}$ we calculated a mean La–O distance in the first hydration shell of 2.52 Å (3 triccaped water molecules at 2.58 Å and 6 prismatic water molecules at 2.50 Å) [10]. The $\mathrm{La(H_2O)}_{8}^{3+}$ and $\mathrm{La(H_2O)}_{10}^{3+}$ stoichiometries are essentially observed at high temperature, and we calculated a mean La–O distance in the first hydration shell of 2.49 and 2.55 Å for $\mathrm{La(H_2O)}_{8}^{3+}$ and $\mathrm{La(H_2O)}_{10}^{3+}$ respectively. As expected, temperature has almost no effect on ADF. This regularity shows that the geometrical distribution for the first hydration shell mainly corresponds to a CN of 9 with the tricapped trigonal prism TTP geometry. While temperature has no effect on the first hydration shell in our temperature range, the radius of the second hydration shell slightly increases above 370 K from 4.65 Å to 4.70 Å at 624 K, whereas the coordination number decreases from 19 at 274 K to 15 at 624 K.

Table 1
Hydration properties of La^{3+} in aqueous solution as a function of the temperature

T (K)	$r^{(1)}_{La-O}$ [a]	$CN^{(1)}$ [b]	θ_{O-La-O} [c]	$MRT^{(1)}$ [d]	$r^{(2)}_{La-O}$ [a]	$CN^{(2)}$ [b]	$MRT^{(2)}$ [d]	D [e]
274	2.52	9.00	70;137	2250	4.65	19.01	9	–
277	2.52	9.01	70;137	1997	4.65	18.99	9	1.74×10^{-9}
290	2.52	9.01	70;137	1422	4.66	18.91	8	1.73×10^{-9}
299	2.52	9.02	70;137	1082	4.65	18.80	8	1.80×10^{-9}
319	2.52	9.02	70;137	713	4.65	18.73	7	2.61×10^{-9}
344	2.52	9.03	70;137	712	4.65	18.55	6	3.10×10^{-9}
370	2.52	9.04	70;136	423	4.65	18.44	5	4.71×10^{-9}
410	2.51	9.06	70;136	244	4.66	17.95	5	3.34×10^{-9}
475	2.51	9.08	69;136	138	4.66	17.54	4	6.27×10^{-9}
508	2.51	9.10	69;136	105	4.68	17.10	4	7.91×10^{-9}
571	2.52	9.11	70;136	59	4.70	16.48	3	10.57×10^{-9}
624	2.51	9.09	70;135	47	4.70	15.52	3	20.03×10^{-9}

[a] First ($r^{(1)}_{La-O}$) and second ($r^{(2)}_{La-O}$) peak maximum of La–O radial distribution functions (in Å).
[b] Coordination number of the first ($CN^{(1)}$) and the second ($CN^{(2)}$) hydration shells.
[c] Peaks of the O–La–O angular distribution functions (in degrees).
[d] Mean residence times of water molecule in the first ($MRT^{(1)}$) and the second ($MRT^{(2)}$) hydration shells (in ps).
[e] Water self-diffusion coefficient ($m^2\,s^{-1}$).

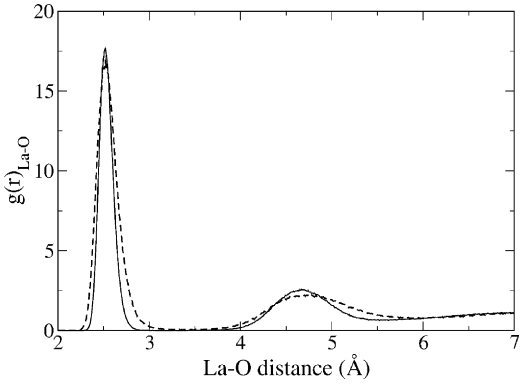

Fig. 1. La–O radial distribution functions at 274 K (solid line) and 571 K (dashed line) and corresponding coordination numbers.

Table 2
Population ratio of the coordination number of the first hydration shell

T (K)	CN = 8	CN = 9	CN = 10	CN = 11
274	1 (<1%)	29865 (100%)	134 (<1%)	0 (0%)
277	1 (<1%)	29638 (99%)	361 (1%)	0 (0%)
290	10 (<1%)	29586 (99%)	404 (1%)	0 (0%)
299	0 (0%)	29435 (98%)	565 (2%)	0 (0%)
319	17 (<1%)	29291 (98%)	692 (2%)	0 (0%)
344	3 (<1%)	28953 (97%)	1044 (3%)	0 (0%)
370	26 (<1%)	28643 (96%)	1331 (4%)	0 (0%)
410	93 (<1%)	27822 (93%)	2085 (7%)	0 (0%)
475	155 (<1%)	27148 (91%)	2695 (9%)	2 (<1%)
508	195 (1%)	26753 (89%)	3049 (10%)	3 (<1%)
571	587 (2%)	25613 (85%)	3796 (13%)	4 (<1%)
624	965 (3%)	25282 (84%)	3738 (13%)	15 (<1%)

The total number of configurations for each simulation is 30000.

Although temperature has virtually no effect on the first hydration shell structural properties, dynamical properties of the first hydration shell are temperature dependent. Increasing temperature decreases the mean residence time (MRT) of water molecules in the first hydration shell from 2250 ps at 274 K to 47 ps at 624 K (Table 1). Note that there are two populations in the tricapped trigonal prism D_{3h} geometry and they have two different residence times consistently with the concerted exchange mechanism as described in Ref. [10]. The number of water exchanges also increases with temperature: we observed 3 events at 274 K, while at 624 K we observed too many exchanges to count them one by one as we did at 274 K. At 624 K we counted 569 passes of water molecules in the first hydration shell during the 3 ns simulation (note that this number of passes is greater than the total number of water molecule, since during 3 ns a water molecule can be more than once in the first hydration shell), while at 274 K we counted 12 passes.

The water self diffusion coefficients increase with temperature (Table 1) from 1.74×10^{-9} (277 K) to $20.03\times10^{-9}\,m^2\,s^{-1}$ (624 K), slightly smaller than experimental values for pure liquid water [27], as expected from the slowing effect of La^{3+} on the water molecules of its hydrating shells.

4.2. Thermodynamic analysis

We interpreted CNs in terms of the corresponding chemical equilibria of Reaction (2). The linearity of the van't Hoff plots (Fig. 3) indicates that the van't Hoff law is a reasonable approximation in our temperature range: this confirms that the heat capacities and the molar volume changes can be neglected, which allows to determine $\Delta_r H^0_{i,T}$ from the van't Hoff plot (Table 3). The uncertainty on $R\ln(K_{i,T})$ is more important at low temperature where fewer water molecule exchanges were observed. For all the studied reactions ($i = 9$–11) the enthalpic contribution ($\Delta_r H^0_{i,298}$) is quite predominant as compared to the entropic contribution ($T\Delta_r S^0_{i,298}$), which is almost within the error bars. Only $\Delta_r H^0_{9,298}$ is negative. $\Delta_r H^0_{i,298}$ increases with i, cer-

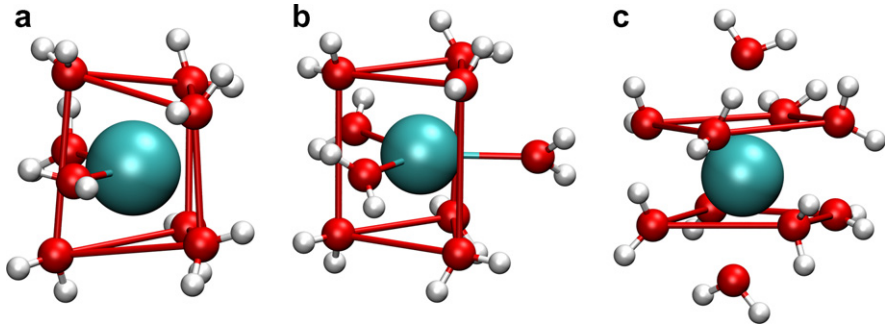

Fig. 2. Some snapshots geometries of the La^{3+} first hydration shell extracted from MD simulation in bulk water: (a) $La(H_2O)_8^{3+}$ in a (6+2) geometry, (b) $La(H_2O)_9^{3+}$ in the 6+3 geometry and (c) $La(H_2O)_{10}^{3+}$ in the $2\times(4+1)$ geometry.

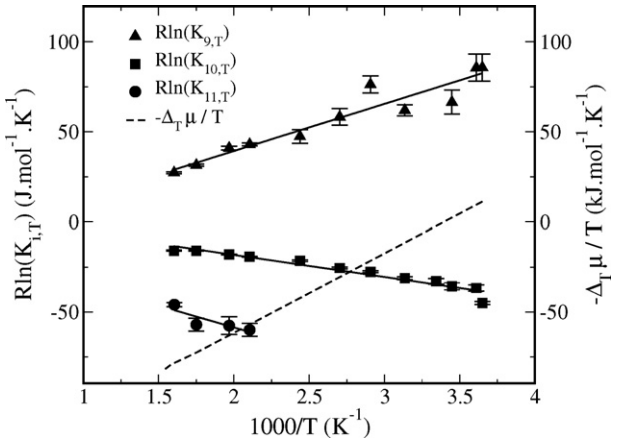

Fig. 3. Van't Hoff plots for equilibrium $La(H_2O)_{(i-1)}^{3+} + H_2O \rightleftharpoons La(H_2O)_i^{3+}$. $-\frac{\Delta_T\mu}{T}$ curve (dashed line) is also shown for comparison.

Table 3
Energies changes for Reactions $M(H_2O)_{i-1}^{3+} + H_2O \rightleftharpoons M(H_2O)_i^{3+}$ × (kJ mol^{-1})

M	i	$\Delta_r H^0_{i,298}$	$-298\ \Delta_r S^0_{i,298}$	$\Delta_r G^0_{i,298}$	$\log(K_{i,298})$
Cm[a]	9	-13.1 ± 0.4	$+7.6 \pm 0.4$	-5.5 ± 0.6	+0.96[e]
Ce[b]	9	−13.00	+9.83	−3.17	+0.68[e]
Ce[c]	9	−15	+10	−5	+0.88
La[d]	9	-26.2 ± 2.8	$+3.9 \pm 2.3$	-22.3 ± 3.6	$+3.9 \pm 0.6$
La[d]	10	$+12.2 \pm 1.0$	-1.9 ± 0.8	$+10.4 \pm 1.4$	-1.8 ± 0.2
La[d]	11	$+24.1 \pm 10.1$	$+3.1 \pm 5.6$	$+27.2 \pm 11.6$	-4.7 ± 11.6

[a] TRLFS – 0.1 mol L^{-1} $HClO_4$ [11].
[b] ^{17}O NMR – 0.033 mol L^{-1} $Ce(ClO_4)_3$ and 0.1 mol L^{-1} $HClO_4$ [14].
[c] Electrostatic model [15].
[d] Present study.
[e] The CN of Ce^{3+} and Cm^{3+} in aqueous solution are 8.8 and 8.9, respectively.

tainly reflecting the over crowding of the first hydration shell. $\Delta_r G^0_{i,298}$ is of the same sign as $\Delta_r H^0_{i,298}$: $\Delta_r G^0_{9,298} < 0$ while $\Delta_r G^0_{i,298} > 0$ for $i > 9$ in the 274–624 K temperature range, reflecting the main CN of 9. Finally, CN is essentially originated in $\Delta_r H^0_{i,298}$ value. This is consistent with the importance of the ionic radii to extrapolate data to others lanthanides [10].

Linear regression through the data points yields $\Delta_r H^0_{9,298} = -26.2 \pm 2.8$ kJ mol^{-1} and $\Delta_r S^0_{9,298} = -13.1 \pm 7.7$ J mol^{-1} K^{-1} for Reaction (2). These thermodynamic parameters are of the same order of magnitude as published values (Table 3), but they are different of about 4–6 kJ mol^{-1} for the entropic contributions. However, questionable assumptions were used to obtain the experimental values [11]. In particular no spectral changes with temperature were assumed for each $M(H_2O)_i^{3+}$ species. Indeed TRLFS observations were interpreted assuming that the TRLFS spectral changes were only originated in the changes of the $Cm(H_2O)_8^{3+}/Cm(H_2O)_9^{3+}$ ratio, *i.e.* no spectral changes with temperature were assumed for each $Cm(H_2O)_i^{3+}$ species [11]. Note that Miyakawa's [15] electrostatic model is based on static calculations of a limited number of geometries for the $Ln(H_2O)_8^{3+}/Ln(H_2O)_9^{3+}$ energy changes.

The temperature dependency of the bulk water term in our system ($\Delta_T\mu$) is more important than the temperature dependency of the concentration ratio between species $(i-1)$ and i (Fig. 3). This certainly illustrates that each species can be modelled by quite rigid clusters only composed of the first hydration shell, whose energy difference does not vary much with temperature, while the second hydration shell and the bulk water terms depend more on temperature. However, this last contribution cancels out to a large extend in energies of reactions.

5. Conclusion

A detailed temperature study of the La^{3+} hydration has been performed by means of molecular dynamics simulations using explicit polarization in the 274–623 K temperature range for the first time to our best knowledge. The present work clearly shows a temperature dependency of the La^{3+} hydration, in particular on the second hydration shell structure and first hydration shell dynamics.

From the $La(H_2O)_{i-1}^{3+}/La(H_2O)_i^{3+}$ equilibrium, thermodynamic parameters ($\Delta_r H^0_{i,298}, \Delta_r S^0_{i,298}$) have been extracted for successive hydration reactions. The $La(H_2O)_{(i-1)}^{3+}/La(H_2O)_i^{3+}$ equilibrium is found to be enthalpy driven. Note that temperature influence is less important on the

$La(H_2O)_{i-1}^{3+}/La(H_2O)_i^{3+}$ concentration ratio than on the chemical potential of bulk water.

Finally, as far as our calculations have shown that the water exchange reactions are enthalpy driven, this is in agreement with the picture of a predominant role of ionic radii in determining Ln^{3+} hydration properties. This encourages us in extending our simple pair potential to the whole lanthanide series – and this is easily feasible with our potential form. Our research is currently going in that direction.

Acknowledgements

We are grateful to Dr. Dominique You for providing us the water densities calculated from Ref. [24], and to Dr. Marie-Pierre Gaigeot and Dr. M. Souaille for helpful discussions and suggestions.

References

[1] L. Helm, F. Foglia, T. Kowall, A.E. Merbach, J. Phys.: Condens. Matter 6 (1994) A132.
[2] T. Kowall, F. Foglia, L. Helm, A.E. Merbach, J. Phys. Chem. 99 (1995) 13078.
[3] T. Kowall, F. Foglia, L. Helm, A.E. Merbach, J. Am. Chem. Soc. 117 (1995) 3790.
[4] T. Kowall, F. Foglia, L. Helm, A.E. Merbach, Chem. Eur. J. 2 (1996) 285.
[5] F.M. Floris, A. Tani, J. Chem. Phys. 115 (2001) 4750.
[6] C. Clavaguéra, R. Pollet, J.M. Soudan, V. Brenner, J.P. Dognon, J. Phys. Chem. B 109 (2005) 7614.
[7] S.R. Hughes, T.-N. Nguyen, J.A. Capobianco, G.H. Peslherbe, Int. J. Mass Spectrom. 241 (2005) 283.
[8] C. Clavaguera, F. Calvo, J.-P. Dognon, J. Chem. Phys. 124 (2006) 074505.
[9] A. Ruas, P. Guilbaud, C. Den Auwer, C. Moulin, J.-P. Simonin, P. Turq, P. Moisy, J. Phys. Chem. A 110 (2006) 11770.
[10] M. Duvail, M. Souaille, R. Spezia, T. Cartailler, P. Vitorge, J. Chem. Phys. 127 (2007) 034503.
[11] P. Lindqvist-Reis, R. Klenze, G. Schubert, T. Fanghänel, J. Phys. Chem. B 109 (2005) 3077.
[12] P. Zanonato, P. Di Bernardo, A. Bismondo, G. Liu, X. Chen, L. Rao, J. Am. Chem. Soc. 126 (2004) 5515.
[13] T. Vercouter, P. Vitorge, B. Amekraz, E. Giffaut, S. Hubert, C. Moulin, Inorg. Chem. 44 (2005) 5833.
[14] G. Laurenczy, A.E. Merbach, Helv. Chim. Acta 71 (1988) 1971.
[15] K. Miyakawa, Y. Kaizu, H. Kobayashi, J. Chem. Soc. 84 (1988) 1517.
[16] M. Souaille, D. Borgis, M.-P. Gaigeot, MDVRY: Molecular Dynamics Program Developed at the University of Evry, for more information please contact Marie-Pierre Gaigeot at gaigeot@ccr.jussieu.fr, 2006.
[17] B.T. Thole, Chem. Phys. 59 (1981) 341.
[18] W.L. Jorgensen, J. Chandrasekhar, J.D. Madura, R.W. Impey, M.L. Klein, J. Chem. Phys. 79 (1983) 926.
[19] R.A. Buckingham, Proc. Roy. Soc. A 168 (1938) 264.
[20] P.J. Hay, W.R. Wadt, J. Chem. Phys. 82 (1985) 270.
[21] W.R. Wadt, P.J. Hay, J. Chem. Phys. 82 (1985) 284.
[22] P.J. Hay, W.R. Wadt, J. Chem. Phys. 82 (1985) 299.
[23] P.C. Hariharan, J.A. Pople, Theor. Chim. Acta 28 (1973) 213.
[24] W. Wagner, A. Pruss, J. Phys. Chem. Ref. Data 31 (2002) 387.
[25] R.D. Shannon, Acta Crystallogr. A 32 (1976) 751.
[26] U. Essmann, L. Perera, M.L. Berkowitz, T. Darden, H. Lee, L.G. Pedersen, J. Chem. Phys. 103 (1995) 8577.
[27] K. Krynicki, C.D. Green, D.W. Sawyer, Faraday Discuss. Chem. Soc. 66 (1978) 199.